

Efficient 2.7- μm emission in Er^{3+} -doped bismuth germanate glass pumped by 980-nm laser diode

Guoying Zhao (赵国营)^{1,2*}, Ying Tian (田颖)^{1,2}, Huiyan Fan (范慧艳)³,
Junjie Zhang (张军杰)¹, and Lili Hu (胡丽丽)¹

¹Key Laboratory of Materials for High Power Laser, Shanghai Institute of Optics and Fine Mechanics,
Chinese Academy of Sciences, Shanghai 201800, China

²Graduate University of Chinese Academy of Sciences, Beijing 100049, China

³SCHOTT Glass Technologies (Suzhou) Co., Ltd., Suzhou 215009, China

*Corresponding author: zhaogy135@126.com

Received January 13, 2012; accepted March 14, 2012; posted online May 16, 2012

An Er^{3+} -doped lead-free bismuth germanate glass is synthesized. Its 2.7- μm emission property is analyzed, and the efficient 2.7- μm emission from the glass is observed under 980-nm laser diode excitation. The prepared glass possesses high spontaneous transition probability (64.8 s^{-1}) and a large calculated emission cross section ($6.61 \times 10^{-21} \text{ cm}^2$) corresponding to the $^4\text{I}_{11/2} \rightarrow ^4\text{I}_{13/2}$ transition. The multiphonon relaxation rate for the excited state $^4\text{I}_{11/2}$ is only 236 s^{-1} . Therefore, the excellent spectroscopic properties and outstanding thermal stability suggest that this glass is a suitable host for developing solid-state lasers operating in the mid-infrared.

OCIS codes: 160.2750, 160.4760, 160.5690.

doi: 10.3788/COL201210.091601.

Over the past several decades, compact solid-state lasers operating in the wavelength region around 2.7 μm have been actively developed because of their applicability in various fields, such as remote sensing, atmosphere pollution monitoring, eye-safe laser radar, and medical surgery^[1–4]. Much effort has been directed to the search for new laser materials in the mid-infrared (MIR) range. Host glass and active ion are two important factors in achieving efficient and high-quality optical devices based on rare-earth ions. Er^{3+} -doped non-oxide glass (such as fluoride and chalcogenide glasses), which is a compact and efficient source of 2.7- μm radiation, has been researched extensively^[5–9]. However, fluoride and chalcogenide glasses have fussy preparation processes and poor thermal stability, chemical durability, and physical and mechanical performance. These disadvantages restrain their wider application in 2.7- μm fibers^[10]. Therefore, MIR laser materials from oxide glass are necessary.

To improve the emission feature of the $\text{Er}^{3+}:^4\text{I}_{11/2}$ excited state, the oxide glass host should have low phonon energy. Among various oxide glasses, bismuth glass shows many significant advantages over other oxide glasses in terms of the fluorescent properties of rare earth. A previous study has shown that bismuth glass has significantly lower phonon energy (MPE of $\sim 440 \text{ nm}^{-1}$) than germanate and tellurite glasses. This property is helpful in reducing the multiphonon relaxation rate for $\text{Er}^{3+}:^4\text{I}_{11/2} \rightarrow ^4\text{I}_{13/2}$ transition^[11]. The large refractive index (~ 2.1) is favorable for obtaining large absorption and emission cross sections. Moreover, bismuth glass exhibits better thermal stability and chemical durability than fluoride and chalcogenide glasses. These characteristics make bismuth glass a suitable host for MIR solid-state lasers. This work aims to investigate the spectroscopic performance of 2.7- μm emission in Er^{3+} -doped bismuth glass, as well as the radiative properties and emis-

sion cross section.

The investigated host bismuth glass had the following composition in cation%: 55BiO_{1.5}-30GeO₂-15NaO_{0.5} (BGNE). The single doping concentration of Er^{3+} in the form of ErF_3 was 2 mol%. Using ErF_3 will induce a positive effect on MIR emission properties of rare earth (RE) ions^[12]. The raw materials were prepared from high-purity Bi₂O₃, GeO₂, Na₂CO₃, and ErF_3 powder. Thirty grams of well-mixed raw materials were placed in an alumina crucible and melted at 1050 °C for 30 min in oxygen atmosphere. Bubbling dry oxygen gas in melts was used to minimize the hydroxyl groups. The melts were quickly poured on a preheated stainless-steel mold and annealed for 2 h near the glass transition temperature (T_g). The annealed sample was fabricated and polished to the size of 20×10×1 (mm) for the optical property measurements.

The characteristic temperatures of the glass sample, including the glass transition temperature T_g , crystallization onset temperature T_x , and crystallization peak temperature T_p were characterized using a differential scanning calorimeter (DSC) (STA449/C, Netzsch) at a heating rate of 10 K/min. The refractive indices were measured at room temperature using a Prism Coupler (Model 2010/M, Metricon). The MIR transmission spectrum was measured using a spectrometer (Nidnet FFIR, Thermo scientific) in the wavenumber range from 1500 to 4000 cm^{-1} . The absorption spectra from 300 to 2000 nm were recorded using a spectrophotometer (Lambda 900 UV/VIS/NIR, Perkin-Elmer) at 1-nm steps. The fluorescence spectra were obtained using a spectrophotometer (TRIA550, Jobin Yvon) with a 980-nm laser diode (LD) as excitation source.

The characteristic temperatures T_g , T_x , and T_p derived from the DSC curve for the host glass are 370, 511, and 527 °C, respectively. The temperature gap ΔT ($T_x - T_g$)

and Hruby's parameter $k_{gl}=(T_p - T_g)/(T_m - T_g)$ are useful in evaluating glass forming ability^[13]. T_m is the melting temperature. The existing thermal stability criterion ΔT and k_{gl} are 147 °C and 0.231, respectively. The two values are larger than those of fluoride and other bismuth glasses^[14,15], indicating that this bismuth germanate glass has good thermal stability.

Figure 1(a) depicts the IR transmittance spectrum of bismuth germanate glass. As shown, the maximum transmittance from 2 500 to 2 900 nm reaches as high as 83.4%. The absorption cut-off edge is up to 6 μm . The small absorption band around 3 250 cm^{-1} is assigned to the stretching vibration of free OH^- groups. Its absorption coefficient α_{OH} is 0.46 cm^{-1} , which is lower than those of other reports^[11,16]. The good infrared transmission of this bismuth germanate glass will benefit its spectroscopic properties in MIR range.

The room-temperature absorption spectrum of the Er^{3+} -doped bismuth germanate glass in the wavelength region from 400 to 1 800 nm is shown in Fig. 1(b). The absorption peaks corresponding to transitions from the ground state $^4\text{I}_{15/2}$ to the excited states are labeled. The Judd–Ofelt (J-O) theory has been extensively employed to determine the radiative properties from the absorption spectrum^[17,18]. The interaction parameters Ω_λ of a ligand field for removing forbidden transition are written as

$$\Omega_\lambda = (2\lambda + 1) \sum_{p,t} A_{t,p}^2 B^2(t,p)(2t + 1) - 1, \quad (1)$$

where $A_{t,p}^2$ is the odd part of the ligand field potential and $B(t,p)$ is the corresponding radial integrated part. Ω_λ can be obtained using the least-squares fitting from the absorption spectra of glasses doped with RE ions. The J-O parameters and experimental and calculated oscillator strengths of Er^{3+} in bismuth germanate glass and various other glass hosts are listed in Table 1. The good agreement between f_{exp} and f_{cal} and the root-mean-square (RMS) deviation δ_{rms} 0.22×10^{-6} indicate reliable calculations. Ω_2 is sensitive to the chemical bonding between RE ions and ligand anions as well as to the asymmetry of local environment around RE ions. Thus, the covalent degree and asymmetry environment of the investigated bismuth germanate glass is stronger than those of fluoride and fluorophosphate glasses. On the other hand, the Ω_4/Ω_6 parameter reflects the stimulated emission property in a laser material^[6]. The relatively high Ω_4/Ω_6 value of the BGNE glass will benefit the radiative transition.

Some important radiative properties were obtained using the J-O parameters, a density of 6.56 g/cm^3 , and a refractive index of 2.11 (Table 1). Further calculation shows that the predicted spontaneous emission probability A for the $\text{Er}^{3+} : ^4\text{I}_{11/2} \rightarrow ^4\text{I}_{13/2}$ transition in the prepared glass is significantly larger than that of other hosts. The corresponding branching ratio β is also larger than those of the three other glasses.

The IR emission spectrum of the Er^{3+} -doped bismuth germanate glass pumped by a 980-nm laser diode (LD) are obtained and shown in Fig. 2. Two specific emission bands of Er^{3+} are observed around 2.7 and 1.5 μm . These bands correspond to the $^4\text{I}_{11/2} \rightarrow ^4\text{I}_{13/2}$ and $^4\text{I}_{13/2} \rightarrow ^4\text{I}_{15/2}$ transitions, respectively. The 2.7- μm emission cross section σ_{em} can be calculated according to the Fuchtbauer–Ladensburg theory and emission spectra^[19,20]. The maximum of the calculated emission cross section in the Er^{3+} -doped bismuth germanate glass at 2 724 nm reaches $6.61 \times 10^{-21} \text{ cm}^2$, which is higher than that of Er^{3+} -doped oxyfluoride glass ceramics ($4.3 \times 10^{-21} \text{ cm}^2$)^[20]. Multiphonon relaxation to a large extent determines the luminescence intensity and radiative transition efficiency. Hence, the multiphonon relaxation rate W_{MPR} can be calculated according to the procedures proposed by Man *et al.*^[21,22]. The W_{MPR} for $\text{Er}^{3+} : ^4\text{I}_{11/2} \rightarrow ^4\text{I}_{13/2}$ in the investigated glass is 236 s^{-1} , which is lower than that of germanates ($1.11 \times 10^4 \text{ s}^{-1}$) and fluorophosphates ($6.53 \times 10^3 \text{ s}^{-1}$)^[22].

To understand the energy transfer mechanism further, we obtained the upconversion spectra of the glass sample under 980-nm excitation (Fig. 3). The intense green light can easily be seen with naked eyes. The involved energy-level diagram and possible energy transfer routes are shown in the inset of Fig. 3. Under 980-nm laser excitation, the $\text{Er}^{3+} : ^4\text{I}_{11/2}$ level is populated. On the one hand, Er^{3+} ions in $^4\text{I}_{11/2}$

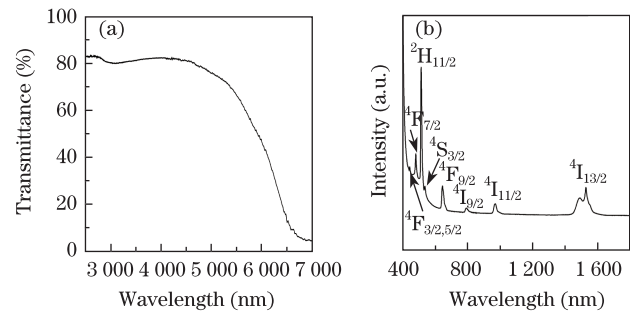


Fig. 1. (a) IR transmittance spectrum and (b) absorption spectrum of Er^{3+} -doped bismuth germanate glass.

Table 1. J-O Parameters, Experimental and Calculated Oscillator Strengths, Spontaneous Emission Probability, and Branching Ratio of Er^{3+} in Various Hosts

Host	Ω_2	Ω_4	Ω_6	Ω_4/Ω_6	Oscillator Strength		A(s^{-1})		Reference
					$[^4\text{I}_{15/2} \rightarrow ^4\text{I}_{11/2}](\times 10^{-6})$		$[^4\text{I}_{11/2} \rightarrow ^4\text{I}_{13/2}]$	$\beta(\%)$	
					f_{exp}	f_{cal}			
Fluoride	3.08	1.46	1.69	0.86	0.851	0.746	29.04	15.89	5
Chalcohalide	6.37	1.41	0.73	1.93			48.4	16.6	6
Fluorophosphate	2.77	1.68	1.47	1.14			24.35	15	9
BGNE	4.71	1.40	0.93	1.51	0.679	0.730	64.8	17.07	this work

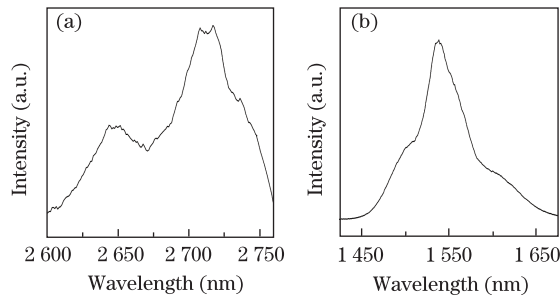


Fig. 2. IR emission spectrum at (a) 2.7 and (b) 1.5 μm of Er^{3+} -doped bismuth germanate glass.

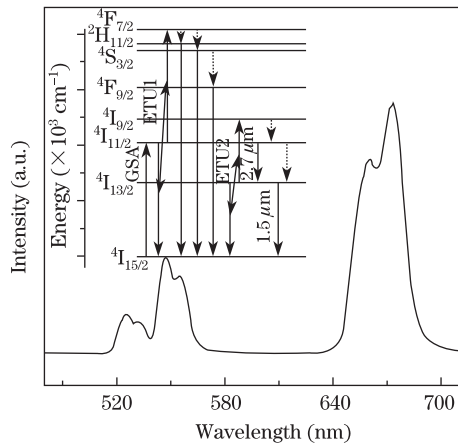


Fig. 3. Upconversion spectrum of Er^{3+} -doped bismuth germanate glass. (Inset) Energy-level diagram of Er^{3+} pumped by 980 nm.

de-excite nonradiatively to $^4\text{I}_{13/2}$ or radiatively to $^4\text{I}_{13/2}$, producing 2.7- μm emission. Then, the relaxation from $^4\text{I}_{13/2}$ level to $^4\text{I}_{15/2}$ yields 1.5- μm emission. On the other hand, Er^{3+} ions in the $^4\text{I}_{11/2}$ level undergo energy transfer upconversion via $^4\text{I}_{11/2} + ^4\text{I}_{11/2} \rightarrow ^4\text{F}_{7/2} + ^4\text{I}_{15/2}$ (ETU1). As a result, the $^4\text{F}_{7/2}$ level is populated. The nonradiative decay happens from $^4\text{F}_{7/2}$ to $^2\text{H}_{11/2}$, $^4\text{S}_{3/2}$, and $^4\text{F}_{9/2}$ because of the small energy gap. Three upconversion emission peaks in the visible range are attributed to the $^2\text{H}_{11/2} \rightarrow ^4\text{I}_{15/2}$, $^4\text{S}_{3/2} \rightarrow ^4\text{I}_{15/2}$, and $^4\text{F}_{9/2} \rightarrow ^4\text{I}_{15/2}$ transitions. The energy transfer upconversion of Er^{3+} ions in $^4\text{I}_{13/2}$ also occurs via $^4\text{I}_{13/2} + ^4\text{I}_{13/2} \rightarrow ^4\text{I}_{9/2} + ^4\text{I}_{15/2}$ (ETU2), which is helpful to the population of the $^4\text{I}_{11/2}$ level and 2.7- μm emission^[23].

In conclusion, efficient emission at 2.7 μm is observed in the Er^{3+} -doped lead-free bismuth germanate glass, which has good thermal stability and higher transmittance around 2.9 μm . This glass also possesses higher spontaneous transition probability (64.8 s^{-1})

and larger emission cross section ($6.61 \times 10^{-21} \text{ cm}^2$) for $\text{Er}^{3+}: ^4\text{I}_{11/2} \rightarrow ^4\text{I}_{13/2}$ transition. The experimental results indicate that the Er^{3+} -doped bismuth germanate glass is a promising candidate for 2.7- μm lasers.

This work was supported by the National Natural Science Foundation of China under Grant No. 60937003.

References

1. R. S. Eng, J. F. Butler, and K. J. Linden, *Opt. Eng.* **19**, 945 (1980).
2. R. Kaufmann, A. Hartmann, and R. Hibst, *J. Dermatol. Surg. Oncol.* **20**, 112 (1994).
3. S. D. Jackson and A. Lauto, *Laser Surg. Med.* **30**, 184 (2002).
4. R. Xu, Y. Tian, L. Hu, and J. Zhang, *Opt. Lett.* **36**, 1173 (2011).
5. Y. Tian, R. Xu, L. Hu, and J. Zhang, *Opt. Mater.* **34**, 308 (2011).
6. H. Lin, D. Chen, Y. Yu, A. Yang, and Y. Wang, *Opt. Lett.* **36**, 1815 (2011).
7. Y. Tian, R. Xu, L. Hu, and J. Zhang, *Opt. Lett.* **36**, 3218 (2011).
8. J. Fan, X. Yuan, R. Li, H. Dong, J. Wang, and L. Zhang, *Opt. Lett.* **36**, 4347 (2011).
9. L. Wen, J. Wang, L. Hu, and L. Zhang, *Chin. Opt. Lett.* **9**, 12601 (2011).
10. Y. Tsang, B. Richards, D. Binks, J. Lousteau, and A. Jha, *Opt. Express* **16**, 10690 (2008).
11. H. Fan, G. Gao, G. Wang, J. Hu, and L. Hu, *Opt. Mater.* **32**, 627 (2010).
12. J. H. Song and J. Heo, *J. Mater. Res.* **21**, 2323 (2006).
13. A. Hruby, *Czech. J. Phys.* **22**, 1187 (1972).
14. D. R. MacFarlane, J. Javorniczky, P. J. Newman, V. Bogdanov, D. J. Booth, and W. E. K. Gibbs, *J. Non-Cryst. Solids* **213–214**, 158 (1997).
15. G. Gao, L. Hu, H. Fan, G. Wang, K. Li, S. Feng, S. Fan, and H. Chen, *Opt. Mater.* **32**, 159 (2009).
16. K. Li, Q. Zhang, G. Bai, S. Fan, J. Zhang, and L. Hu, *J. Alloys Compd.* **504**, 573 (2010).
17. B. R. Judd, *Phys. Rev.* **127**, 750 (1962).
18. G. S. Ofelt, *J. Chem. Phys.* **37**, 511 (1962).
19. S. Payne, L. Chase, L. Smith, W. Kway, and W. Krupke, *IEEE J. Quantum Electron.* **28**, 2619 (1992).
20. V. K. Tikhomirov, J. Méndez-Ramos, V. D. Rodríguez, D. Furniss, and A. B. Seddon, *Opt. Mater.* **28**, 1143 (2006).
21. S. Man, S. Wong, E. Pun, and Po. Chung, *J. Opt. Soc. Am. B.* **21**, 313 (2004).
22. X. Zou and T. Izumitani, *J. Non-Cryst. Solids* **162**, 68 (1993).
23. P. S. Golding, S. D. Jackson, T. A. King, and M. Pollnau, *Phys. Rev. B* **62**, 856 (2000).